Identification of unique bile acid-metabolizing bacteria from the microbiome of centenarians

Kenya Honda (kenya@keio.jp)
Keio University School of Medicine https://orcid.org/0000-0001-8937-9835
Yuko Sato
Keio University School of Medicine https://orcid.org/0000-0002-2177-5820
Koji Atarashi
Keio University School of Medicine https://orcid.org/0000-0001-5422-0736
Damian Plichta
Broad Institute https://orcid.org/0000-0002-6555-2557
Yasumichi Arai
Keio University School of Medicine
Satoshi Sasajima
Keio University School of Medicine
Sean Kearney
Massachusetts Institute of Technology
Wataru Suda
RIKEN Center for Integrative Medical Sciences
Kozue Takeshita
Keio University School of Medicine
Takahiro Sasaki
Health Sciences University of Hokkaido
Shoki Okamoto
Keio University School of Medicine
Ashwin Skelly
Keio University School of Medicine https://orcid.org/0000-0002-1565-3376
Yuki Okamura
Keio University School of Medicine
Hera Vlamakis
Broad Institute https://orcid.org/0000-0003-1086-9191
Youxian Li
RIKEN Center for Integrative Medical Sciences
Takeshi Tanoue
Keio University School of Medicine
Hajime Takei

Junshin Clinic Bile Acid Institute

Hiroshi Nittono

Junshin Clinic Bile Acid Institute

Seiko Narushima

RIKEN Center for Integrative Medical Sciences

Junichiro Irie

School of Medicine, Keio University https://orcid.org/0000-0003-2662-4121

Hiroshi Itoh

Department of Endocrinology, Metabolism and Nephrology, School of Medicine, Keio University

Kyoji Moriya

The University of Tokyo

Yuki Sugiura

Keio University School of Medicine

Makoto Suematsu

Keio University https://orcid.org/0000-0002-7165-6336

Nobuko Moritoki

Keio University School of Medicine

Shinsuke Shibata

Keio University School of Medicine https://orcid.org/0000-0002-1185-9043

Dan Littman

New York University School of Medicine

Michael Fischbach

UCSF https://orcid.org/0000-0003-3079-8247

Masahira Hattori

Waseda University

Tsuyoshi Murai

Health Sciences University of Hokkaido

Ramnik Xavier

Massachusetts General Hospital https://orcid.org/0000-0002-5630-5167

Nobuyoshi Hirose

Keio University School of Medicine

Biological Sciences - Article

Keywords: gut microbiota, centenarians, bile acids

Posted Date: December 2nd, 2020

DOI: https://doi.org/10.21203/rs.3.rs-115113/v1

Version of Record: A version of this preprint was published at Nature on July 29th, 2021. See the published version at https://doi.org/10.1038/s41586-021-03832-5.

Identification of unique bile acid-metabolizing bacteria from the microbiome of centenarians

Yuko Sato[1,3,5,§], Koji Atarashi[1,3,5,§], Damian R. Plichta[4,§], Yasumichi Arai[2], Satoshi Sasajima[1,5], Sean M. Kearney[1,3], Wataru Suda[3], Kozue Takeshita[1,5], Takahiro Sasaki[6], Shoki Okamoto[1], Ashwin N. Skelly[1], Yuki Okamura[1], Hera Vlamakis[4], Youxian Li[3], Takeshi Tanoue[1,3,5], Hajime Takei[7], Hiroshi Nittono[7], Seiko Narushima[1,3], Junichiro Irie[8], Hiroshi Itoh[8], Kyoji Moriya[9], Yuki Sugiura[10], Makoto Suematsu[10], Nobuko Moritoki[11], Shinsuke Shibata[11], Dan R. Littman[12,13], Michael A. Fischbach[14], Masahira Hattori[3], Tsuyoshi Murai[6], Ramnik J. Xavier[4,15], Nobuyoshi Hirose[2], Kenya Honda[1,3,5,*]

[1]Department of Microbiology and Immunology, Keio University School of Medicine, Tokyo, Japan.

[2]Centre for Supercentenarian Medical Research, Keio University School of Medicine, Tokyo, Japan.

[3]RIKEN Center for Integrative Medical Sciences, Yokohama, Japan.

[4]Infectious Disease and Microbiome Program, Broad Institute of MIT and Harvard, Cambridge, MA, USA.

[5]JSR-Keio University Medical and Chemical Innovation Center, Tokyo, Japan.

[6]School of Pharmaceutical Sciences, Health Sciences University of Hokkaido, Hokkaido, Japan.

[7]Junshin Clinic Bile Acid Institute, Tokyo, Japan.

[8]Department of Internal Medicine, Division of Endocrinology, Metabolism and Nephrology, Keio University School of Medicine, Tokyo, Japan.

[9]Department of Infection Control and Prevention, The University of Tokyo, Tokyo, Japan.

[10]Department of Biochemistry, Keio University School of Medicine, Tokyo, Japan.

[11]Electron Microscope Laboratory, Keio University School of Medicine, Tokyo, Japan.

[12]The Kimmel Center for Biology and Medicine of the Skirball Institute, New York University School of Medicine, New York, NY, USA.

[13]Howard Hughes Medical Institute, New York, NY, USA.

[14]Department of Bioengineering, Stanford University, Stanford, CA, USA.

[15]Center for Computational and Integrative Biology, Massachusetts General Hospital and Harvard Medical School, Boston, MA, USA.

[§]These authors equally contributed to this work.

*To whom correspondence should be addressed.

Kenya Honda; Tel: +81-3-5363-3768; Fax: +81-3-5361-7658; Email: kenya@keio.jp

Abstract

Centenarians, or individuals who have lived more than a century, represent the ultimate model of successful longevity associated with decreased susceptibility to ageing-associated illness and chronic inflammation[1–3]. The gut microbiota is considered to be a critical determinant of human health and longevity[4–8]. Here we show that centenarians (average 107 yo) have a distinct gut microbiome enriched in microbes capable of generating unique secondary bile acids, including iso-, 3-oxo-, and isoallo-lithocholic acid (LCA), as compared to elderly (85-89 yo) and young (21-55 yo) controls. Among these bile acids, the biosynthetic pathway for isoalloLCA had not been described previously. By screening 68 bacterial isolates from a centenarian's faecal microbiota, we identified *Parabacteroides merdae* and *Odoribacteraceae* strains as effective producers of isoalloLCA. Furthermore, we generated and tested mutant strains of *P. merdae* to show that the enzymes 5α-reductase (5AR) and 3β-hydroxysteroid dehydrogenase (3βHSDH) were responsible for isoalloLCA production. This secondary bile acid derivative exerted the most potent antimicrobial effects among the tested bile acid compounds against gram-positive (but not gram-negative) multidrug-resistant pathogens, including *Clostridioides difficile* and vancomycin-resistant *Enterococcus faecium*. These findings suggest that specific bile acid metabolism may be involved in reducing the risk of pathobiont infection, thereby potentially contributing to longevity.

Main

The microbiome has long been recognized as a key player in determining the health status of ageing individuals through its role in controlling digestive functions, bone density, neuronal activity, immunity, and resistance to pathogen infection[9–13]. Microbial consortia in elderly individuals often show increased interindividual variability and reduced diversity, and are thus being linked to immunosenescence, chronic systemic inflammation, and frailty[6,14]. An integrated understanding of the dynamic balance and functions of microbial members with respect to ageing is essential for establishing a strategy toward rational manipulation of the microbiota for restoring and/or maintaining tissue homeostasis and overall health.

Centenarians (aged 100 years and older) are known to be less susceptible to age-related diseases including hypertension, diabetes, obesity, and cancer[3,15]. Moreover, centenarians have likely survived periods of hunger and several bouts with infectious diseases such as influenza, tuberculosis, shigellosis, and salmonellosis[16]. It has been postulated that there are centenarian-specific members of the gut microbiota which, rather than representing a mere consequence of ageing, might actively contribute to maintaining homeostasis, resilience, and healthful ageing[4–6,8]. In this study, we aimed

to identify symbiotic, beneficial bacteria in the gut microbiota of centenarians that may contribute to resistance to pathogen infection and other environmental stresses.

Microbiome signature of centenarians

We recruited a cohort consisting of three age groups: centenarian (n = 160), elderly (n = 112), and young (n = 44). All centenarians were recruited as part of the Japan Semi-supercentenarian Study[15], with most living in nursing homes (85.0%) and the remainder at home (9.4%) or in hospitals (5.6%) (**Table S1**). Centenarians generally reported reduced activities of daily living (ADL) and mini-mental state examination (MMSE) scores, along with reduced red blood cell counts and serum albumin (**Extended Data Fig**. **1a-c** and **Table S1**). Consistent with the paradigm that ageing is accompanied by chronic inflammation secondary to decreased barrier integrity and immunosenescence[9,12,13], a subset of centenarians showed signs of low-grade inflammation as evidenced by elevated serum C-reactive protein and faecal lipocalin (**Extended Data Fig**. **1c, d)**. Nevertheless, the majority of centenarians were free of chronic diseases such as obesity, diabetes, hypertension, and cancer, and the prevalence of these diseases was not significantly increased as compared to the elderly group (**Extended Data Fig**. **1e, f** and **Table S1**). We collected faecal samples from the three groups to characterize the microbiome by both 16S ribosomal RNA (rRNA) amplicon and whole metagenome shotgun sequencing. Principal coordinate analysis (PCoA) based on the Bray-Curtis distance revealed significant differences in microbiota composition between centenarians and both control groups (PERMANOVA FDR $P < 0.05$, **Fig. 1a**). At the phylum level, we observed a significant enrichment of Proteobacteria and Synergistetes, a moderate enrichment of Verrucomicrobia, and a depletion of Actinobacteria in centenarians as compared to controls (**Fig**. **1c** and **Extended Data Fig. 2**), partially in agreement with previous centenarian studies including that of the Sardinian cohort[8]. Such expansions of Proteobacteria are a frequent finding in patients with inflammatory bowel disease (IBD)[17]; however, in contrast to the reduced microbial α-diversity commonly observed in IBD patients, centenarians had on average a higher Shannon diversity index compared to young controls (**Fig. 1b**). Moreover, the microbiota composition of centenarians was distinct from that of IBD patients, as evidenced by differential clustering in PCoA analyses (**Extended Data Fig. 3a**).

Several taxa displayed differential relative abundances in centenarians versus control groups (**Fig. 1d-f** and **Extended Data Fig. 3b-d**), which we categorized into three signatures based on trajectory with age: (i) The first signature included taxa whose abundance was increased or decreased with age (**Fig. 1d**). For example, *Eubacterium siraeum* and undefined Firmicutes species (msp_161, 213) were most abundant in centenarians, followed by the elderly and then the young controls,

whereas *Blautia wexlerae* displayed the opposite trend, being most abundant in young controls, followed by the elderly and finally the centenarians. *Alistipes shahii* was comparably enriched in both the elderly and centenarian groups as compared to young controls. These findings are in alignment with previous studies that suggest the relative abundances of these taxa reflect adaptation to ageing, and may be related to physical activity, environment, and diet[4–6,8]. (ii) The second signature included taxa whose abundance was similar in centenarians and young controls, but distinct from the elderly (**Fig. 1e**). These species might reflect the maintenance of youth or possess reverse-ageing effects. Notably, *Ruminococcus gnavus* and *Eggerthella lenta* were part of this signature, as they were comparably abundant in both centenarians and young controls. Interestingly, these species have been implicated in bile acid metabolism, and likely participate in the biosynthesis of iso-bile acids in the host gut[18]. (iii) The third signature included centenarian-specific taxa whose abundance was significantly different between centenarians and both the elderly and young control groups, but not between these two control groups (**Fig. 1f**). Here, *Alistipes, Parabacteroides*, *Bacteroides*, and *Clostridium* species, as well as *Methanobrevibacter*, a predominant archaeon in the human gut, were specifically enriched in centenarians as compared to the other groups. One of the most abundant species in centenarians was *Clostridium scindens*, which is known to possess the relatively rare 7α-dehydroxylation capacity needed to convert primary into secondary bile acids[19,20]. In contrast, key butyrate producers such as *Faecalibacterium prausnitzii*, *Eubacterium rectale*, *and Roseburia intestinalis* were selectively depleted in centenarians (**Fig. 1f**). Some of these observations are in agreement with the Sardinian study, in which centenarians exhibited a decreased relative abundance of *F. prausnitzii* and *E. rectale*, and an increase in *M. smithii*[8].

We also collected stool from the lineal descendants and siblings of centenarians and analysed them by 16S rRNA sequencing (n = 22 from 14 centenarians, 48-95 yo, **Extended Data Fig. 3** and **Table S1**). Some bacterial species, such as *Phascolarctobacterium faecium* and *Alistipes putredinis*, were more abundant in centenarians and their family members as compared to the other groups (**Extended Data Fig. 3d**). Enrichment of these taxa in centenarians and their lineal descendants may be due to host genetics, lifestyle, and diet; for example, consumption of cruciferous vegetables has been reported to favour expansion of the aforementioned taxa[21].

Centenarians have a unique bile acid profile

We next assessed the faecal metabolite profile of centenarians as compared to elderly and young controls. We first analysed faecal short-chain fatty acids (SCFAs) and found decreased levels of both propionic and butyric acid in centenarians (**Extended Data Fig. 4a**). In contrast, branched-SCFAs like isobutyric and isovaleric acid, as well as ammonium, were elevated in centenarians

(**Extended Data Fig. 4a-b**). These metabolic alterations are consistent with previous observations[4,5,8] and may be attributable to the simultaneous depletion of SCFA-producers, such as *R. intestinalis* and *F. prausnitzii*[22] (**Fig. 1f**), and enrichment of protein-fermenting organisms, such as *A. putredinis*[23] (**Fig. 1f**). This increase in amino acid-utilizing bacteria is likely a consequence of the reduced upper intestinal proteolytic capacity commonly observed in centenarians. Moreover, faecal pH was significantly higher in centenarians than controls (**Extended Data Fig. 4c**), which may be due in part to the lower SCFA concentrations and reduced gastric juice production characteristic of ageing.

Given the enrichment of species potentially capable of metabolizing bile acids in centenarians, we next focused on faecal bile acid distribution. Primary bile acids are synthesized from cholesterol in the liver, conjugated to either glycine or taurine, and secreted into bile[24,25]. These primary bile acids are then deconjugated and biotransformed into a variety of secondary bile acids by the gut microbiota[19,25]. The predominant biotransformation is the 7α-dehydroxylation of primary bile acids [cholic acid (CA) and chenodeoxycholic acid (CDCA)], thereby converting them into secondary bile acids [deoxycholic acid (DCA) and lithocholic acid (LCA)]. Microbiota-mediated bile acid metabolism consists of multiple redox reactions catalysed by enzymes encoded by bile-acid-inducible (*bai*) operon genes: *BaiB*, *BaiCD*, *BaiA2*, *BaiE*, *BaiF*, and *BaiH*[19,26] (**Extended Data Fig. 5a)**. In addition to the 7α-dehydroxylation, bile acids can undergo oxidation and epimerization to generate oxo- (keto-), iso- (3β-hydroxy), allo- (5α-H-), as well as *cis*- and *trans*-forms[25] (**Extended Data Fig. 5a**). Metagenomic analysis of our cohorts identified an increase in the relative abundance of *bai* operon gene homologues in centenarians (**Fig. 1g**), though this trend was not apparent in the Sardinian cohort (**Extended Data Fig. 6**).

To characterize the bile acid profile of centenarians, we implemented a highly sensitive, targeted liquid chromatography-tandem mass spectrometry (LC-MS/MS) method. In pilot studies, we found that 95 of 132 examined bile acids were minor components (<0.5 μmol/g) of centenarians' faeces. We thus selected the remaining 37 relevant bile acid compounds for follow-up quantitative analysis (**Fig. 2a** and **Table S2**). Although total bile acid load in filtered, weight-normalized stool suspensions was not significantly different between groups, centenarians showed a unique distribution of faecal bile acids (**Fig. 2a-c** and **Extended Data Fig. 7**). For example, centenarians exhibited lower levels of primary bile acids with increased levels of CDCA metabolites (**Fig. 2d-f**). In particular, the levels of isoLCA, 3-oxoLCA, and isoalloLCA were significantly elevated in centenarians, whereas they were comparably low in the elderly and young control groups, suggesting that this enrichment is not simply a byproduct of ageing (**Fig. 2a, f**). Furthermore, the concentrations of isoLCA, 3-oxoLCA, and isoalloLCA were positively associated with faecal pH (**Extended Data Fig. 4d**), potentially implying that their enrichment in centenarians may reflect changes in diet and

digestive function, as well as consequent changes in the intestinal luminal metabolome. Such an intestinal milieu may promote the expansion of certain bacterial species and/or the expression of enzymes involved in the production of isoLCA, 3-oxoLCA, and isoalloLCA. Alternatively, intestinal colonization by isoLCA-, 3-oxoLCA-, and isoalloLCA-producing bacteria may causally affect other members of the gut microbiota and their metabolic processes.

Identification of isoLCA-, 3-oxoLCA-, and isoalloLCA-producing bacterial strains

We set out to identify bacterial strains and enzymes responsible for the biosynthesis of isoLCA, 3-oxoLCA, and isoalloLCA in centenarians' microbiota. A previous report demonstrated that 3-oxoDCA can be generated from 3-oxo-Δ^4-DCA (also termed 3-oxo-4,5-dehydro-DCA) by hydrogenation across the C4-C5 double bond such that the C5 hydrogen is in the β position (**Extended Data Fig. 5b**). This reaction is mediated by a 3-oxo-5β-steroid 4-dehydrogenase (also termed 5β-reductase, 5BR) encoded by the *BaiCD* gene, which is reported to be carried by a small number of *Clostridium* species including *C. scindens* and *C. hylemonae*[26,27]. It has additionally been reported that *E. lenta* and *R. gnavas* can generate 3-oxoDCA from DCA, and isoDCA from 3-oxoDCA, by the actions of 3α-hydroxysteroid dehydrogenase (3αHSDH) and 3βHSDH, respectively[18]. Thus, we hypothesized that 3-oxoLCA and isoLCA are produced in a manner similar to 3-oxoDCA and isoDCA, via the actions of 5BR, 3αHSDH, and 3βHSDH (**Fig. 2g** and **Extended Data Fig. 5a**). On the other hand, the biosynthetic pathway leading to isoallo-bile acid generation had not been previously determined. We predicted that isoalloLCA might be generated from 3-oxo-Δ^4-LCA by the sequential action of a 5α-reductase (5AR) homologue and 3βHSDH, through a 3-oxoalloLCA intermediate. 5AR is known to mediate the conversion of testosterone into 5α-dihydrotestosterone by hydrogenating across the C4-C5 double bond, thereby forcing the A and B steroid rings into a planar (*trans*) conformation[28] (**Extended Data Fig. 5c**). We reasoned that 3-oxoalloLCA (a *trans*-bile acid) might arise from 3-oxo-Δ^4-LCA via an analogous pathway. We also predicted that the subsequent transformation of 3-oxoalloLCA to isoalloLCA might use a 3βHSDH, mirroring the previously characterized conversion of 3-oxoDCA to isoDCA[18] (**Fig. 2g** and **Extended Data Fig. 5b**).

In order to validate our pathway predictions and identify isoLCA-, 3-oxoLCA-, and isoalloLCA-producing bacterial strains, we followed up on a supercentenarian (CE91, over 110 yo) who displayed no major abnormalities in a blood test and showed high levels of faecal iso-, 3-oxo-, and isoallo-LCA (**Fig. 2a**). We cultured faecal samples from CE91 *in vitro* in a variety of media and analysed bacterial colonies by 16S rRNA gene sequencing to elaborate a consortium of 68 unique

strains, which roughly recapitulated the microbiota structure of CE91 (**Fig. 3a** and **Table S3**). We then incubated individual isolates at pH 7 or pH 9 with either CDCA, LCA, or 3-oxo-Δ^4-LCA as starting substrates. Culture supernatants were collected after 48 hr and bile acids were quantified by LC-MS/MS (**Fig. 3b, c** and **Extended Data Fig. 8**). Incubation with CDCA did not result in production of iso-, 3-oxo-, or isoallo-LCAs in any of the cultures, though *C. scindens* strains 59-60 (St59-60) and *C. hylemonae* St63 were able to produce LCA, albeit at low levels (**Extended Data Fig. 8a, b**), in line with previous reports[27]. When cultured with LCA, *Gordonibacter pamelaeae* St32 and *E. lenta* St33-35 were found to produce 3-oxoLCA and isoLCA (**Fig. 3b** and **Extended Data Fig. 8c, d**), implying their carriage of 3αHSDH and 3βHSDH as predicted in a previous study[18]. In addition, *Raoulibacter timonensis* St30-31 and *Lachnospiraceae* spp. St57 were also capable of transforming LCA into 3-oxoLCA, suggesting that these species possess 3αHSDH, similar to *E. lenta*. When 3-oxo-Δ^4-LCA was used as a substrate, 3-oxoLCA accumulated to high levels in the supernatants of *Hungatella hathewayi* St54-55 and *Lachnospiraceae* spp. St62 cultures (**Fig. 3c** and **Extended Data Fig. 8e, f**), suggesting that these strains possess 5BR. Similarly, isoLCA was generated from 3-oxo-Δ^4-LCA at high levels in *Clostridium innocuum* St51 and *Lachnospiraceae* spp. St58 cultures (**Fig. 3c** and **Extended Data Fig. 8e, f**), suggesting carriage of 5BR and 3βHSDH. It is noteworthy that *Parabacteroides distasonis* St4-5 converted LCA to 3-oxoLCA and further to 3-oxo-Δ^4-LCA (**Fig. 3b** and **Extended Data Fig. 8c, d**), as well as 3-oxo-Δ^4-LCA to isoLCA and LCA (**Fig. 3c** and **Extended Data Fig. 8e, f**), suggesting that these strains possess 3αHSDH, 3βHSDH, and 5BR. Collectively, at least 12 among 68 strains were capable of robustly generating 3-oxoLCA, and 8 were able to generate isoLCA from either LCA or 3-oxo-Δ^4-LCA.

Strikingly, after incubation with 3-oxo-Δ^4-LCA, a marked accumulation of isoalloLCA was observed in the cultures of *Parabacteroides merdae* St3, *Odoribacter laneus* St19, *Odoribacteraceae* spp. St21-24, and to a lesser degree in those of *Bacteroides dorei* St6-7 (**Fig. 3c** and **Extended Data Fig. 8e, f**), suggesting that these strains harbour both 5AR and 3βHSDH activities. Additionally, *Parabacteroides goldsteinii* St1-2*, Bacteroides thetaiotaomicron* St9*, B. uniformis* St10-13, *Alistipes finegoldii* St15-16, *A. onderdonkii* St17-18, and *O. laneus* St20 cultures all displayed a substantial accumulation of presumed intermediate 3-oxoalloLCA, but little to no isoalloLCA (**Fig. 3c** and **Extended Data Fig. 8e, f**), likely due to carriage of 5AR but lack or insufficient activity of 3βHSDH in these culture conditions. Therefore, a total of 20 Bacteroidales strains (St1-24 excluding St4, 5, 8, and 14) were found to be capable of transforming 3-oxo-Δ^4-LCA into 3-oxoalloLCA, 8 of which were able to robustly generate isoalloLCA. Of note, incubation at pH 9 (representative of centenarians' gut environment) enhanced the accumulation of 3-oxoalloLCA, isoalloLCA, isoLCA, and 3-oxoLCA as

compared to that at pH 7 (**Extended Data Fig. 8**), suggesting that alkaline pH stress may promote the activity or expression of enzymes involved in the production of these bile acids.

5AR- and 3βHSDH-mediated transformation of 3-oxo-Δ^4-LCA to isoalloLCA

To further validate our predicted biosynthetic pathway, and in particular the hypotheses that 3-oxo-Δ^4-LCA conversion to 3-oxoLCA and isoLCA is mediated by 5BR and 3α-/3β-HSDH, and that isoalloLCA generation is mediated by 5AR and 3βHSDH, we sequenced the genomes of all 68 isolates by integrating Miseq and PacBio platforms (**Table S3**). Querying these genome sequences revealed carriage of 3αHSDH genes by *Eggerthella* strains (**Fig. 3e**), in line with a previous report[18]. *P. distasonis* St4, 5 were also found to have putative 3αHSDH genes, consistent with the above *in vitro* evaluation of bile acid metabolism. Additionally, sequences orthologous to human 5AR (*steroid 5 alpha-reductase 1*, *SRD5A1*) were identified in 21 Bacteroidales strains with >30% amino acid sequence similarity (magenta in **Fig. 3d-e**, **Extended Data Fig. 9**, and **Extended Data Fig. 10a**). We next assessed genes directly adjacent to the predicted 5AR loci. In all 21 strains, we found clusters of genes functionally related to bile acid metabolism, including sequences annotated as NADH:flavin oxidoreductase, which we predicted to be 5BR (blue in **Fig. 3d-e**, **Extended Data Fig. 9**, and **Extended Data Fig. 10b**). We also identified sequences annotated as short-chain dehydrogenase (SDR), which we predicted to be 3βHSDH. These SDR sequences comprised two groups: group I sequences (green) showed high similarity (>40%) to *P. merdae* St3 3βHSDH, whereas group II sequences (purple) were closely related to one another but not to *P. merdae* St3 3βHSDH (**Fig. 3d-f**, **Extended Data Fig. 9**, and **Extended Data Fig. 10c**). In addition, there were sequences presumably encoding bile acid transporters near the gene clusters (**Extended Data Fig. 9**). We found that carriage of putative 5AR and 3βHSDH genes was clearly related to 3-oxoalloLCA and/or isoalloLCA production from 3-oxo-Δ^4-LCA, except in the case of St8 (**Fig. 3c, e**).

To further elucidate the relevant biosynthetic pathways, we deepened our *in vitro* screen of the 24 Bacteroidales isolates' bile acid transformation capabilities by incubating each with either 3-oxoalloLCA, 3-oxoLCA, or isoLCA (**Extended Data Fig. 11a-c**). The observed patterns of bile acid transformation were largely consistent with our predicted pathway, although there was substantial substrate specificity and strain-to-strain variation in transformation efficiency. For instance, *P. merdae* St3, *P. distasonis* St4-5, and *B. dorei* St7, and *Odoribacteraceae* St21 all had strong 3βHSDH activities, reflected by simultaneous high isoalloLCA production from 3-oxoalloLCA (**Extended Data Fig. 11a**) and isoLCA production from 3-oxoLCA (**Extended Data Fig. 11b**), whereas several other strains such as *B. dorei* St6 and *B. uniformis* St10-13 showed less efficient biotransformation

despite carriage of putative 3βHSDH genes (**Extended Data Fig. 11a, b**). The strength of 5BR activity also differed among the strains: *P. distasonis* St4-5 and *B. dorei* St7 effectively transformed 3-oxoLCA to 3-oxo-Δ^4-LCA, while other strains showed moderate to weak activities (**Extended Data Fig. 11b**). *Porphyromonas somerae* St14 lacked putative 5AR and 3βHSDH genes but was able to generate isoalloLCA from 3-oxoalloLCA nonetheless (**Extended Data Fig. 11a**), suggesting that it carries a strain-specific gene with 3βHSDH activity. To examine whether isolates carrying different genes were capable of cooperatively metabolizing bile acids, we cocultured *E. lenta* St34 (a 3αHSDH and 3βHSDH encoder) or *P. distasonis* St4 (a 3αHSDH, 3βHSDH, and 5BR encoder) with *P. merdae* St3 or *Odoribacteraceae* St21 (5BR, 5AR, and 3βHSDH encoders) in the presence of LCA. All combinations resulted in cooperative production of isoalloLCA, with *E. lenta* St34 and *P. merdae* St3 coculture giving the highest yield (**Extended Data Fig. 11d**). Collectively, although there were strain-dependent differences in enzymatic activity, substrate specificity, and gene location, the Bacteroidales gene clusters identified above likely contribute to the cooperative production of bile acids and may be responsible, at least in part, for the unique faecal bile acid profile observed in centenarians.

To further confirm the roles of 5AR and 3βHSDH in microbiota-mediated bile acid metabolism, we set out to generate mutant strains of *P. merdae* and *Odoribacteraceae*. Although a lack of genetic tools hampered the introduction of targeted mutations in *Odoribacteraceae* strains, we were able to successfully generate three *P. merdae* St3 mutants lacking genes encoding putative 5AR (PM3806), 3βHSDH (PM3804), or 5BR (PM3805) via conjugation[29] (**Extended Data Fig. 12**). As expected, when incubated with 3-oxo-Δ^4-LCA, *P. merdae*Δ5AR failed to produce either 3-oxoalloLCA or isoalloLCA, whereas *P. merdae*Δ3βHSDH was able to generate 3-oxoalloLCA but not isoalloLCA (**Fig. 3f**). Consistently, when incubated with 3-oxoalloLCA, *P. merdae*Δ5AR generated isoalloLCA in a manner similar to the wild-type parental strain, whereas *P. merdae*Δ3βHSDH did not (**Fig. 3f**). *P. merdae*Δ3βHSDH additionally failed to convert 3-oxoLCA into isoLCA, confirming that 3βHSDH can utilize both *trans*- and *cis*- bile acids as substrates. *P. merdae*Δ5BR produced isoalloLCA from 3-oxo-Δ^4-LCA or 3-oxoalloLCA but showed a defect in transforming 3-oxoLCA into 3-oxo-Δ^4-LCA (**Fig. 3f**). Together, these results corroborate the involvement of 5AR, 3βHSDH, and 5BR in the production of isoalloLCA, 3-oxoLCA, and isoLCA by the human gut microbiota.

Bactericidal effects of isoalloLCA against gram-positive pathogens

Secondary bile acids are known to play important roles in several biological contexts, such as modulation of host metabolic and immune responses (including the induction of regulatory T cells)[25,30–35] and prevention of intestinal pathogen expansion[36–39]. In particular, DCA, LCA, and isoLCA have been implicated in inhibiting the growth of *Clostridioides difficile*[36,40], which is currently classified as one of the most urgent antibiotic resistance threats[41]. Thus, we next investigated whether 3-oxoLCA and isoalloLCA share this capacity to inhibit *C. difficile* growth. We incubated *C. difficile* 630 with various concentrations of isoLCA, 3-oxoLCA, isoalloLCA, 3-oxoalloLCA, LCA, DCA, or vehicle control and used optical density measurements to track growth over time *in vitro*. Strikingly, isoalloLCA potently inhibited the growth of *C. difficile* 630. The minimal inhibitory concentration required to prevent ≥90% growth (MIC90) in WCA medium was 2.0 μM, far below that of the other bile acids tested (**Fig. 4a, b** and **Extended Data Fig. 13a, b**). Potent growth inhibition by isoalloLCA was also observed in toxigenic *C. difficile* VPI10463 and vancomycin-resistant *Enterococcus faecium* (VRE) (**Fig. 4a, b** and **Extended Data Fig. 13a, b)**. Scanning and transmission electron microscopy revealed that isoalloLCA was bactericidal, producing morphologic and ultrastructural alterations including collapse, swelling, and multiple cross walls in *C. difficile* 630 and VRE (**Fig. 4c**). These patterns of damage are reminiscent of those induced by β-lactam antibiotics[42]. Co-culturing with *Odoribacteraceae* St21 in conjunction with 3-oxo-Δ^4-LCA supplementation resulted in significant *C. difficile* 630 and VRE growth inhibition, similar to that observed with isoalloLCA treatment (**Fig. 4d**). In contrast, bacteriostatic effects were not observed when co-culturing was performed with *C. innocuum* St51 (an isoLCA producer) or *P. distasonis* St4 (an isoLCA and LCA producer).

We then examined the effect of isoalloLCA on other gram-positive pathogens, including methicillin-resistant *Staphylococcus aureus* (MRSA), *Streptococcus dysgalactiae* subsp. *equisimilis* (SDSE), *Clostridium perfringens*, *Streptococcus pyogenes*, *Streptococcus sanguinis,* and *Bacillus cereus*, as well as on gram-negative pathogens, including *Klebsiella pneumoniae*, *Escherichia coli*, *Salmonella enterica*, *Proteus vulgaris*, and *Proteus mirabilis*. *S. aureus* is a prominent skin pathogen, though it often colonizes the intestine and is known to be resistant to most bile acids[43]. IsoalloLCA strongly inhibited growth of all gram-positive pathogens tested, including *S. aureus*, with MIC90 values ranging from 0.5 to 3 μM in WCA and from 3 to 6.25 μM in BHI medium (**Fig. 4a, b** and **Extended Data Fig. 13a, b**). In contrast, all members of our gram-negative pathogen panel were resistant to isoalloLCA, even at the highest concentration tested (50 μM) (**Fig. 4a, b** and **Extended Data Fig. 13a, c**). Taken together, these results suggest that isoalloLCA exerts strong bactericidal/bacteriostatic effects specifically on gram-positive pathogens, suggesting that it may interfere with the bacterial cell wall.

Effects of isoalloLCA on the commensal gut microbiota

Gut metabolites are encountered not only by enteric pathogens, but also by commensals, and as such we proceeded to investigate how isoalloLCA affects common members of the human microbiota. A total of 42 prevalent gut microbiota members, consisting of both gram-positive and gram-negative species, were selected from our culture collection, and each was incubated with increasing concentrations of isoalloLCA in WCA and BHI media. IsoalloLCA did not appreciably affect the growth of most gram-negative commensals such as *Bacteroides* (**Fig. 4e** and **Extended Data Fig. 14a**). In contrast, it substantially interfered with the growth of gram-positive commensals (**Fig. 4e** and **Extended Data Fig. 14a**). However, MIC90 values for commensal strains were generally higher than those for pathogens, and scanning electron microscopy revealed that commensals' cell wall structures [*C. sporogenes, C. indolis,* and *C.* HGF2 (*innocuum*)] were preserved when incubated with 2.5 μM isoalloLCA (1.25x MIC90 for *C. difficile*) (**Extended Data Fig. 14b**). In particular, *Lactobacillus* strains were highly resistant to the inhibitory effects of isoalloLCA (**Fig. 4e**). Moreover, culturing commensal strains in peptone- and amino acid-rich BHI conferred increased resistance to isoalloLCA as compared to culturing in WCA medium, whereas pathogens generally remained sensitive irrespective of media (**Fig. 4a, e** and **Extended Data Fig. 15**). These results indicate that although the concentration at which isoalloLCA exerts bactericidal effects on gram-positive bacteria varies substantially depending on environmental conditions, pathogens consistently remain more sensitive than commensals.

To further evaluate the effects of isoalloLCA within the context of a complex, normal gut flora, we incubated human faecal microbiota from young, healthy volunteers with isoalloLCA, 3-oxoLCA, LCA, or vehicle control, and analysed the shift in bacterial composition by 16S rRNA gene sequencing. Although α-diversity was not significantly affected, isoalloLCA induced broad changes in microbial community structure that were evident at the phylum level (**Fig. 4f, g**). We observed a pronounced reduction in gram-positive species like *Clostridium*, *Faecalibacterium*, *Bifidobacterium*, and *Streptococcus*, along with a corresponding increase in gram-negative species like *Bacteroides* and *Alistipes*, following incubation with isoalloLCA as compared to other bile acid compounds (**Fig. 4g**). These results are consistent with the increased relative abundance of *Bacteroides* and *Alistipes* seen in centenarians' gut microbiota, and suggest that isoalloLCA can directly impact the structure of intestinal microbial communities.

Finally, having confirmed that 5AR, 5BR, and 3βHSDH play critical roles in the production of unique secondary bile acid derivatives, we returned to the metagenome sequence data of Japanese centenarians to identify additional species that carry these genes. 5AR, 5BR, and 3βHSDH gene

clusters were identified in 35 species (all Bacteroidales) (**Extended Data Fig. 16a**). We evaluated the abundance of these species in relation to faecal concentrations of isoLCA, 3-oxoLCA, and isoalloLCA. We observed a significant positive correlation between isoalloLCA levels and several *Alistipes* sp., *Bacteroides cellulosilitycus*, *B. intestinalis*, and *P. goldsteinii*; these species were also positively associated with isoLCA and 3-oxoLCA concentrations (**Extended Data Fig. 16b**). In contrast, *Bacteroides vulgatus* and *Bacteroides ovatus* were significantly negatively associated with the three tested secondary bile acids. *O. laneus* showed significant or moderate positive correlations with 3-oxoLCA, isoLCA, and isoalloLCA, and we did not observe significant associations between *P. merdae* and these bile acids (**Extended Data Fig. 16b**). These results suggest that expression and activity of the identified genes may be regulated via complex species-specific and intestinal milieu-dependent mechanisms and likely involve interbacterial- and bacteria-host interactions *in vivo*.

Discussion

In the present study, we identified centenarian-specific gut microbiota signatures and defined bacterial species and genes/pathways that promote the generation of isoLCA, 3-oxoLCA, and isoalloLCA. It has been reported that isoalloLCA induces T_{reg} cells and that 3-oxoLCA and isoLCA suppresses T helper 17 (T_H17) cells, and as such the accumulation of these bile acids may protect against overexuberant immune responses and inflammation (ref.[30] and Jun Huh and A. Sloan Devlin, personal communication). Consistent with this notion, centenarians who participated in this and previous studies[1–3] were largely unafflicted by chronic diseases, such as metabolic disease and cancer, which are associated with aberrant activation of immune system and immunosenescence[12]. In addition to the previously reported anti-inflammatory properties of isoalloLCA, we found that it also exerts a very strong antibacterial effect against gram-positive pathogens. Several reports have demonstrated that bile acids contribute to protection against enteropathogenic infection[36,44,45]. To our knowledge, isoalloLCA is one of the most potent antimicrobial agents selective against gram-positive microbes, including multidrug-resistant pathogens. Although more research is needed to elucidate the molecular mechanism by which isoalloLCA disrupts bacterial cell wall structure, our findings suggest that isoalloLCA may be a potential factor contributing to longevity by promoting colonization resistance against gram-positive pathogens. Regardless of whether the increase in isoalloLCA-, isoLCA-, and 3-oxoLCA-producing microbes is a consequence of ageing or a contributor to longevity, these bile acids could be used as biomarkers to monitor health conditions and predict life expectancy. Moreover, we could exploit the unique bile acid-metabolizing capabilities of the bacterial strains identified in this study to rationally manipulate the bile acid pool and ultimately ameliorate infectious

diseases caused by gram-positive pathogens including antibiotic-resistant *C. difficile*, VRE, and MRSA.

Methods

Human sample collection

Faecal sample collection and blood tests from young, elderly, centenarians, and lineal relatives of centenarians were carried out following protocol approved by the Institution Review Board (IRB) of Keio University School of Medicine (code 20150075 for young healthy donors; 20160297 for elderly cohorts (as a part of Kawasaki Aging and Wellbeing project); and 20022020 for centenarians and lineal relatives of centenarians (as a part of The Japan Semi-supercentenarian Study[15]). Faecal sample collection of IBD patients were carried out under the IRB of Osaka City University (code 2413). Informed consent was obtained from each donor prior to participation. All experiments adhered to the regulations mandated by these review boards. All study procedures were performed in compliance with the relevant ethical regulations. The Japan Semi-supercentenarian Study[15] and Kawasaki Aging and Wellbeing project are registered in the University Hospital Medical Information Network Clinical Trial Registry as observational studies (ID: UMIN 000040447 and UMIN000026053).

Metagenomic sequencing and 16S rRNA gene pyrosequencing of human stool samples

Faecal samples were suspended in an equal volume of PBS containing 20% glycerol and 10 mM EDTA and stored at -80 ºC until use. After thawing, 100 μL of faecal suspension was gently mixed and incubated in 800 μL TE10 (10mM Tris-HCl, 10 mM EDTA) buffer containing RNase A (final concentration of 100 μg/mL, Invitrogen) and lysozyme (final concentration of 15 mg/mL, Sigma) for 1 hr at 37 ºC. Purified achromopeptidase (final concentration of 2,000 U/mL, Wako) was added and further incubated for 30 min at 37 ºC. SDS (final concentration of 1%) and proteinase K (final concentration of 1 mg/mL, Roche) was further added to the mixture and incubated for 1 hr at 55 ºC. High molecular weight DNA was extracted with phenol:chloroform:isoamyl alcohol (25:24:1 at pH 7.9), precipitated with isopropanol (equal volume to the aqueous phase), washed with 1 mL of 70% ethanol, and gently resuspended in 30 μL of TE buffer.

The 16S rRNA sequencing was performed using MiSeq according to the Illumina protocol. PCR was performed using 27Fmod 5'-AGRGTTTGATYMTGGCTCAG-3'and 338R 5'-TGCTGCCTCCCGTAGGAGT-3' to the V1−V2 region of the 16S rRNA gene. Amplicons generated from each sample (~330bp) were purified using AMPure XP magnetic beads (Beckman Coulter). DNA was quantified using a Quant-iT Picogreen dsDNA assay kit (Invitrogen) and Infinite M Plex plate reader (Tecan), then stored at 4 ºC. The pooled amplicon library was sequenced using a MiSeq Reagent Kit v2 (500 cycles) and Miseq sequencer (Illumina, 2 x 250bp paired-end reads). Two paired-end reads were merged using the fastq-join program based on overlapping sequences. Reads with an average quality value of <25 and inexact matches to both universal primers were filtered out. Both primer sequences were trimmed off and 3,000 quality filter-passed reads were rearranged in descending order according to the quality value and then clustered into OTUs with a 97% pairwise-identity cutoff using the UCLUST program v5.2.32[46]. Taxonomic assignment of each OTU was made via searching by similarity against the Ribosomal Database Project (RDP) and the National Center for Biotechnology Information (NCBI) genome database using the GLSEARCH program.

Metagenomic sequencing libraries were prepared from 2 ng of input DNA using the Nextera XT DNA Library Preparation kit (Illumina) according to the manufacturer's recommended protocol. Libraries were pooled

by equal volume and insert sizes and concentrations for each pooled library were determined using an Agilent Bioanalyzer DNA 1000 kit (Agilent Technologies). Sequencing was performed on an Illumina NovaSeq 6000 with 151bp paired-end reads to yield ~10 million paired-end reads per sample. Data was analysed using the Broad Picard Pipeline, which includes de-multiplexing and data aggregation (https://broadinstitute.github.io/picard). The quality control for the metagenomic data was conducted using Trim Galore! to detect and remove sequencing adapters (minimum overlap of 5bp) and KneadData v0.7.2 to remove human DNA contamination and trim low-quality sequences (HEADCROP:15, SLIDINGWINDOW:1:20), retaining reads that were at least 50bp long. Metagenomic reads were assembled individually for each sample into contigs using MEGAHIT[47], followed by an open reading frame prediction with Prodigal[48] and retaining predicted genes that had both a start and a stop codon. A non-redundant gene catalogue was constructed by clustering predicted genes based on sequence similarity at 95% identity and 90% coverage of the shorter sequence using CD-HIT[49,50]. Reads were mapped to the gene catalogue with BWA requiring a unique, strong mapping with at least 95% sequence identity over the length of the read[51], counted (count matrix) and normalized to transcripts per kilobase million (TPM matrix) using in-house scripts. Count matrix served as an input for binning genes into metagenomic species pan-genomes (core and accessory genes) using MSPminer with default settings[52]. We represented the abundance of every metagenomic species (MSP) in a sample as a median TPM for 30 top representative core genes reported by MSPminer. Assembled genes were annotated at species, genus, and phylum levels with NCBI RefSeq (version May 2018) as described previously[53]. To annotate phylogenetically MSPs that had no match to any species from NCBI RefSeq we used Phylophlan with default settings[54]. α-diversities were calculated using Shannon index and β-diversity was calculated using Bray-Curtis dissimilarity based on relative abundances at species levels (Vegan package in R). The non-redundant gene catalogue was queried using USEARCH ublast[53] with proteins in the *bai* operon of *C. scindens*[26] or proteins in the bacterial isolates reported here as 5AR, 5BR, 3βHSDH I, or 3βHSDH II to identify and annotate homologous proteins with at least 40% identity and 80% coverage to the query sequence. An identical processing pipeline has been applied to the dataset describing the gut microbiome in Sardinian centenarians[8].

In the subsequent analysis, we only used samples with at least 4 million reads after the quality control step. Additionally, we discarded samples that were collected while the subject was undergoing any antibiotic treatment. To test differential abundance of species or phyla and differences in the Shannon diversity index, we employed linear random effects modelling (centenarians *vs.* young or elderly controls) or fixed effects modelling (elderly *vs.* young controls), as implemented in the lmer and lm functions in R. Furthermore, for analysis of species differential abundance, we restricted the analysis to MSPs present in at least 10% of samples, zeros were replaced by half of the smallest non-zero measurement on a per-feature basis and $\log_{10}$ transformation was applied on the relative abundances for normality. Linear modelling included fixed effect covariates: sex (male or female) and cohort information (centenarian, elderly, or young); random effect included subject information to account for more than one sample among a few centenarians. The permutational multivariate analysis of variance (PERMANOVA analysis as implemented in adonis function in the R package Vegan was applied to the Bray-Curtis dissimilarity to identify the correlation between age group (centenarian, elderly, young) and sex information and the composition of the gut microbiome as a whole.

Faecal bile acid quantification using LC-MS/MS

Accurately weighed 2 mg of freeze-dried faecal samples were homogenized in 2 mL of 0.2 N NaOH by

ultrasonication for 10 min in a screw-cap glass vial containing 10 μL of deuterium-labelled internal standards (d_4-CA, d_4-GCA, d_4-TCA, d_4-GCDCA, d_4-TCDCA, d_5-CDCA-3S, d_5-GCDCA-3S, and d_5-TCDCA-3S, 20 nmol/mL for d_4-CA and 10 nmol/mL for the rest of compounds). After incubation for 2 hr at room temperature, pH was adjusted to 9.0 using 8 N HCl, mixed with 200 μL of 0.5 M EDTA/0.5 M Tris and 50 μL of 600 U/mL proteinase K (Kanto Chemical Inc.), followed by overnight incubation at 37 ºC. The solution was transferred onto a solid-phase extraction cartridge (Agilent Bond Elut C18, 500 mg/6 mL, preconditioned with 5 mL of methanol and 15 mL of water). The cartridge was washed with 7 mL of water and captured bile acids were eluted with 4 mL of 90% ethanol. After solvent evaporation, the remaining residue was dissolved in 1 mL of 50% ethanol and 5 μL was injected to LC/ESI-MS/MS (LC-MS8050 tandem mass spectrometer, equipped with an ESI probe and Nexera X2 ultra-high-pressure liquid chromatography system; Shimadzu). A separation column, InertSustain C18 (150 mm × 2.1 mm ID, 3 μm particle size; GL Sciences Inc.), was utilized at 40 °C. A mixture of 10 mM ammonium acetate and acetonitrile was used as the eluent and the separation was carried out by linear gradient elution at a flow rate of 0.2 mL/min. The mobile phase composition was gradually changed as follows: ammonium acetate-acetonitrile (86:14, v/v) for 0.5 min, (78:22, v/v) for 0.5-5 min, (72:28, v/v) for 5-28 min, (46:54, v/v) for 28-55 min, (2:98, v/v) for 55-66 min, and (2:98, v/v) for 4 min. The total run time was 70 min. To operate the LC/ESI-MS/MS, the following MS parameters were used: spray voltage; 3,000 V, heating block temperature; 400 °C, nebulizing gas flow; 3 L/min, drying gas flow; 10 L/min, heating gas flow; 10 L/min, interface temperature 300 °C, collision gas (argon) pressure; 270 kPa, collision energy; 13-80 eV, all in the negative ion MRM mode. Samples were analysed and quantified using LabSolutions Insight LC-MS software (Shimadzu).

Faecal SCFA, pH, and ammonia measurement

Faecal SCFA concentration was determined by GC-MS (Shimadzu QP2020 system with a flame ionization detector), equipped with PAL RTC autosampler (CTC Analytics). Helium was used as the carrier gas and fused silica capillary columns 30 m x 0.25 mm coated with 0.25 μm film thickness were used. The injection port temperature was set to 250 °C. The initial oven temperature was held at 60 °C for 2 min and then raremped to 330 °C at a rate of 15 °C per minute. MS parameters were set to: ion source temperature at 200 °C, interface temperature at 280 °C, and loop time of 0.3 sec. For the GC-MS measurement, 50 μL of faecal samples with a concentration of 0.5 μg/μL and 20 μg/μL prepared in ethanol were mixed with 10 μL of acetic acid- d_4 (80 μM). Using PAL RTC autosampler, 4-(4, 6-Dimethoxy-1, 3, 5-triazin-2-yl)-4methylmorpholinium (DMT-MM) and n-octylamine (10 μL of each reagent at a concentration of 80 μM) were added to each faecal samples and reacted for 9 hr prior to injection into GC-MS. Samples were analysed and quantified using LabSolutions Insight GC-MS software (Shimadzu).

Faecal pH was measured from the supernatant from 0.1 mg/μL of faecal suspension in distilled water using a pH meter (Horiba Ltd.). From the same faecal suspension, faecal ammonia level was quantified using enzymatic ammonia ELISA assay kit (Abcam) according to the manufacture's protocol.

Isolation of bacterial strains from a centenarian

A faecal sample from a supercentenarian (CE91, Japanese, female, age >110 years) was suspended in equal volume (w/v) of PBS containing 20% glycerol, snap-frozen in liquid nitrogen, and stored at -80 °C until use. 200 μL of thawed faecal suspension was serially diluted with PBS and 100 μL was seeded onto nonselective [Brucella agar plate with haemin, Vitamin K1, lysed rabbit blood and defibrinated sheep blood (BHK-RS), Kyokuto] and selective

agar plates [for gram-negative bacteria: Paramomycin and vancomycin supplemented BHK, Kyokuyo and for Clostridial bacteria: Oxoid Reinforced Clostridial (RC) Agar, Thermofisher] and grown inside an anaerobic chamber (Coy Laboratory Products) under anaerobic conditions (80% N_2, 10% H_2, and 10% CO_2) at 37 °C. Individual colonies emerged after 72 hr and up to 10 days of incubation were picked. Isolated strains were identified by PCR amplification of the 16S rRNA gene region with universal primers (27Fmod: 5'-AGRGTTTGATYMTGGCTCAG-3', 1492R: 5'-GGYTACCTTGTTACGACTT-3') for Sanger sequencing and using the NCBI genome database. Individual isolates in the culture collection were given species name with >98.0% of 16S rRNA sequence homology, family name with >94.5% similarity and order name with >86.5% similarity. Bacterial isolates were cryo-preserved in 20% glycerol in optimal culture broth at -80 °C.

***In vitro* screening of microbial bile acid metabolism**

Under anaerobic conditions, isolated bacteria strains were cultured together with 50 μM of CDCA, 3-oxo-Δ^4-LCA, or LCA to screen for their bile acid metabolism in a 96-deep well plate (Treff Lab) covered with a gas-permeable membrane (Breathe-easier™, Diversified Biotech). 20 μL of bacterial culture in exponential to stationary phase was inoculated into 1 mL of Wilkins-Chalgren Anaerobe (WCA, Thermofisher) media adjusted to pH 7 (using MOPS buffer solution, Dojindo) or pH 9 (TAPS buffer solution, Dojindo). Several bacterial strains required growth in RC or WCA media supplemented with additional nutrients. *Ruminococcaceae* St42-43 and 45, *Clostridiales* St47, and *Lachnospiraceae* St56 were cultured in RC, while *Phascolarctobacterium faecium* St52-53 were cultured in RC medium supplemented with sodium succinate (20 mmol/L). For *Akkermansia muciniphila* St26-27, WCA medium supplemented with ammonium chloride (1.0 g/L), L-cysteine (1.0 g/L), vitamin K (0.5 mg/L), haemin (5 mg/L), and 0.29% volatile fatty acid solution (based on DSMZ 1611 YCFA modified medium) was used. *Alistipes finegoldii* St16, *Campylobacter ureolyticus* St25, *Christensenellaceae* St36-37, and *Ruminococcaceae* St44 were culture in WCA medium supplemented with 4% salt solution (0.2 g/L calcium chloride, 0.2 g/L magnesium sulphate, 1g/L dipotassium hydrogen phosphate, 1 g/L potassium dihydrogen phosphate, 10 g/L sodium hydrogen carbonate, and 2 g/L sodium chloride), ammonium chloride (1.0 g/L), L-cysteine (1.0 g/L), vitamin K (0.5 mg/L), haemin (5 mg/L), sodium acetate (1.0 g/L), sodium formate (0.15 g/L), sodium fumarate (0.15 g/L), sodium thioglycolate (0.3 g/L), 1% ATCC vitamin solution, and 1% ATCC Trace element solution. For *Methanobrevibacter smithii* St67-68, the above modified WCA medium was further supplemented with sodium bicarbonate (0.25 g/L), sodium sulphide (0.05 g/L), and sodium formate (1.36 g/L)[55]. After 48 hr of anaerobic incubation at 37 °C, culture supernatants were collected and stored at -20 °C until sample preparation for the analysis.

For sample preparation, 100 μL of culture supernatant was transferred into a screw-cap glass vial containing 10 μL of deuterium-labelled internal standards (d_4-CA, d_4-CDCA, and d_4-LCA, 1 nmol/mL each). 400 μL of water was added and sonicated for 10 min, then applied onto the solid-phase extraction cartridge (Agilent Bond Elut C18, 100 mg/1 mL, preconditioned with 1 mL of methanol and 3 mL of water). The cartridge was washed with 1 mL of water and captured bile acids were eluted with 1 mL of 90% ethanol. After solvent evaporation, the remaining residue was dissolved in 100 μL of 50% ethanol, of which 5 μL of the solution was injected to LC/ESI-MS/MS (LC-MS8040 tandem mass spectrometer, equipped with an ESI probe and Nexera X2 ultra-high-pressure liquid chromatography system; Shimadzu). A separation column, InertSustain C18 (150 mm × 2.1 mm ID, 2 μm particle size; GL Sciences Inc.), was utilized at 40 °C. Mixture A (10 mM ammonium acetate, 0.01% formic acid, and 20% acetonitrile) and mixture B (30% acetonitrile and 70% methanol) were used as the eluent, and the separation was

carried out by linear gradient elution at a flow rate of 0.2 mL/min. The mobile phase composition was gradually changed as follows: Mixture A:B (80:20, v/v) for 0.1 min, (48:52, v/v) for 0.1-1 min, (30:70, v/v) for 1-27 min, (0:100, v/v) for 27-27.1 min, (0:100, v/v) for 27.1-33 min, (80:20, v/v) for 33-33.1 min, and (80:20 v/v) for 33.1-83 min. The total run time was 38 min. To operate the LC/ESI-MS/MS, the following MS parameters were used: spray voltage; 3,000V, heating block temperature; 400 °C, nebulizing gas flow; 3 L/min, drying gas flow; 15 L/min, interface temperature 300 °C, collision gas (argon) pressure; 230 kPa, collision energy; negative (11 to -35 eV); and positive (-16 to -19 eV) ion modes. Samples were analysed and quantified using LabSolutions Insight LC-MS software (Shimadzu).

Bacterial whole-genome sequencing

The extracted genomic DNA of 68 isolated strains was sheared to yield DNA fragments. The genome sequences were determined by the whole-genome shotgun strategy using PacBio Sequel and Illumina MiSeq sequencers. The library of the Illumina Miseq 2 x 300bp paired-end sequencing was prepared using TruSeq DNA PCR-Free kit (target length = 550bp) and all the MiSeq reads were trimmed and filtered with a >20 quality value (QV) using FASTX-toolkit (hannonlab.cshl.edu/fastx_toolkit). The library of the PacBio Sequel sequencing was prepared using SMRTbell template prep kit 2.0 (target length = 10 - 15kbp) without DNA shearing. After removal of internal control and adaptor trimming by Sequel, the error correction of the trimmed reads was performed using Canu (v1.8) with additional options (corOutCoverage = 10,000, corMinCoverage = 0, corMhapSensitivity = high). *De novo* hybrid assembly of the filter-passed MiSeq reads and the corrected Sequel reads were performed using Unicycler (v0.4.8), which contained checks for overlapping and circularization to generate circular contigs. The gene prediction and annotation of the generated contigs were performed using the Rapid Annotations based on Subsystem Technology (RAST) server[56] and Prokka software tool[57]. Default parameters were used unless otherwise specified.

Mutant generation

The deletion mutants (Δ5AR, Δ5BR, and Δ3βHSDH) of *P. merdae* St3 were generated by conjugation-mediated plasmid transfection and selection of double-crossover resolvents with a rhamnose-inducible ssBfe1 cassette[29]. Approximately 2kb sequences flanking the coding region were amplified by PCR (PCR primers used in this study are listed in Table S4) and assembled into the PstI and SalI sites of the suicide vector pLGB30 using HiFi DNA Assembly (NEB) as per the manufacturer's protocol. 1 μL aliquots of each reaction were transformed into electro-competent *E. coli* MFDpir[58]. Transformants were conjugated with *P. merdae* St3 as follows. The donor (*E. coli* MFDpir) and recipient (*P. merdae* St3) strains were cultured in LB and BHI media, respectively, to an OD_{600} of 0.5 and mixed at a ratio of 1:1. The mixture was dropped onto a BHI agar plate and incubated anaerobically at 37 °C for 16 hr. Transconjugants were selected on BHI agar plates containing tetracycline (6 μg/mL). Subsequently, to select for loss of plasmid from the genome by a second crossover, transconjugants were plated on M9 agar supplemented with 0.25% (wt/vol) glucose, 50 mg/L L-cysteine, 5 mg/L haemin, 2.5 μg/L vitamin K1, 2 mg/L $FeSO_4 \cdot 7H_2O$, 5 μg/L vitamin B12, and 10 mM rhamnose. Successful deletions were confirmed by PCR and Sanger sequencing.

Bacterial growth inhibition assays

Clostridioides difficile strain 630 (ATCC BAA-1382), *Clostridioides difficile* VPI 10463 (ATCC 43255),

vancomycin-resistant *Enterococcus faecium* (ATCC 700221), *Streptococcus dysgalactiae* subsp. *equisimilis* (ATCC 12394), carbapenemase-resistant *Klebsiella pneumoniae* (ATCC BAA-1705), and *Salmonella enterica* subsp. *enterica* (ATCC 14028) were purchased from American Type Culture Collection, ATCC. *Clostridium perfringens* (JCM 1290^T), *Bacillus cereus* (JCM 2152^T), methicillin-resistant *Staphylococcus aureus* (JCM 16555), *Streptococcus pyogenes* (JCM 5674^T), *Streptococcus sanguinis* (JCM 5708^T), *Proteus mirabilis* (JCM 1669^T), and *Proteus vulgaris* (JCM 20013) were purchased from Japan Collection of Microorganisms, JCM. Adherent invasive *Escherichia coli* was a kind gift from Prof. Nicolas Banich.

For gut commensals, *Clostridium scindens* (ATCC 35704^T), *Clostridium sporogenes* (ATCC 15579), *Dorea formicigenerans* (ATCC 27755^T), *Ruminococcus lactaris* (ATCC 29176 ^{T}), *Bacteroides fragilis* (ATCC 25285^T), *Clostridium indolis* (JCM 1380^T), *Clostridium hiranonis* (JCM 10541^T), *Clostridium hylemonae* (JCM 10539^T), *Clostridium nexile* (JCM 31500^T), *Clostridium butyricum* (JCM 1391^T), *Dorea longicatena* (JCM 11232^T), *Eubacterium hallii* (JCM 31263), *Streptococcus thermophilus* (JCM 17834^T), *Ruminococcus gnavus* (JCM 6515^T), *Anaerotruncus colihominis* (JCM 15631^T), *Blautia producta* (JCM 1471^T), *Blautia obeum* (JCM 31340), *Bifidobacterium bifidum* (JCM 1254), *Bifidobacterium breve* (JCM 1192^T), *Bifidobacterium longum* subsp. *longum* (JCM 1217^T), *Lactobacillus casei* (JCM 1134^T), *Lactobacillus paragasseri* (JCM 1130), *Lactobacillus reuteri* (JCM 1112^T), *Collinsella aerofaciens* (JCM 10188^T), *Roseburia intestinalis* (JCM 17583^T), *Eggerthella lenta* (JCM 9979^T), *Bacteroides caccae* (JCM 9498^T), *Bacteroides finegoldii* (JCM 13345^T), *Bacteroides intestinalis* (JCM 13265^T), *Bacteroides ovatus* (JCM 5824^T), *Bacteroides stercoris* (JCM 9496^T), *Parabacteroides johnsonii* (JCM 13406^T), and *Prevotella copri* (JCM 13464^T) were obtained from ATCC and JCM. Previously described T_{reg} inducing strains[59] from our laboratory were also included in the commensal panel; *Clostridium symbiosum* (VE202-16), *Clostridium ramosum* (VE202-18), *Clostridium bolteae* (VE202-7), and *Flavinofractor plautii* (VE202-3). In addition, *Hungatella hathewayi*, *Eubacterium rectale*, and *Alistipes putredinis* isolated from human faeces in our laboratory were used. *Clostridium* HGF2 (*innocuum*) HM287 was obtained through BEI Resources, NIAID, NIH as part of the Human Microbiome Project: *Clostridium* sp., Strain HGF2, HM-287.

From fresh colonies grown on BHK blood agar plates (Kyokuto), a primary suspension adjusted to OD_{600} of 0.63 was prepared in WCA medium. Subsequently, the secondary suspension was prepared by diluting 100 μL of primary suspension into a total of 2.4 mL of medium. 10 μL of secondary suspension was inoculated to a total of 200 μL of medium containing varying concentrations (3.175, 6.25, 12.5, 25, or 50 μM) of bile acids; DCA, LCA, 3-oxoLCA, 3-oxoalloLCA, isoLCA, alloLCA, or isoalloLCA. The growth of bacteria was monitored every 0.5-1 hr by OD_{600} measurement using a microplate reader (Sunrise Thermo, Tecan) set at 37 °C with a 60 sec shaking before each time point and PLATEmanager v5/S software for the data collection. For determining the minimal inhibitory concentration (MIC), 10 μL of secondary suspension was inoculated into a total of 200 μL of medium containing 0.25 to 50 μM of isoalloLCA.

Electron microscopy (EM)

Bacterial cultures incubated with or without isoalloLCA were collected after 5 hr incubation for EM samples. For scanning electron microscopy (SEM), 10-30 μL of culture was spotted on the Nano percolator membrane (JEOL) and fixed in freshly prepared 2.5% glutaraldehyde solution. After overnight fixation at 4 ºC, samples were washed in 0.1 M phosphate buffer (pH 7.4, Muto Pure Chemicals), fixed with 1.0% osmium tetroxide (TAAB Laboratories) for 2 hr at 4 ºC, and treated with a series of increasing concentrations of ethanol. Samples were dried up with a

critical point dryer (CPD300, Leica Biosystems) and coated with about 2 nm thickness of osmium using a conductive osmium coater (Neoc-ST, Meiwafosis). SEM images were acquired using the SU6600 (Hitachi High Tech) at electron voltage of 5 keV.

For transmission electron microscopy (TEM), microbial pellets were prepared by centrifugation (13,000 rpm, 2 min) from 25 mL bacterial cultures. Pellets were fixed with 2.5% glutaraldehyde solution overnight at 4 ºC. After washing with 0.1 M phosphate buffer, samples were fixed with 1.0% osmium tetroxide for 2 hr at 4 ºC, washed in distilled water, and embedded into low gelling temperature Type VII-A agarose (Sigma-Aldrich). Samples were dehydrated by a series of increasing concentrations of ethanol to absolute ethanol, soaked with acetone (Sigma-Aldrich), with n-butyl glycidyl ether (Okenshoji Co., Ltd.), graded concentration of Epoxy resin with n-butyl glycidyl ether, and also with 100% Epoxy resin (100 g Epon was composed of 27.0 g MNA, 51.3 g EPOK-812, 21.9 g DDSA, and 1.1 mL DMP-30, all from Okenshoji Co., Ltd.) for 48 hr at 4 ºC. Polymerization of pure Epoxy resin was completed for 72 hr at 60 ºC. The ultra-thin sections (70 nm) were prepared on copper grids (Veco Specimen Grids, Nisshin-EM) with an ultramicrotome (Leica UC7, Leica Biosystems), and stained with uranyl acetate and lead citrate for 10 min each. TEM images were obtained using the JEM-1400plus (JEOL) at electron voltage of 80-100 keV.

Culturing human faeces with bile acids

Human faecal culture was conducted in 96-deep well plates (Treff Lab) using stool samples obtained from young and healthy donors (filtered and resuspended in 20% glycerol for cryo-preservation). 5 mg of stool was inoculated into 1 mL of WCA medium supplemented with 4% salt solution (0.2 g/L calcium chloride, 0.2 g/L magnesium sulphate, 1 g/L dipotassium hydrogen phosphate, 1 g/L potassium dihydrogen phosphate, 10 g/L sodium hydrogen carbonate, and 2 g/L sodium chloride), ammonium chloride (1.0 g/L), L-cysteine (1.0 g/L), vitamin K (0.5 mg/L), haemin (5 mg/L), sodium acetate (1.0 g/L), sodium formate (0.15 g/L), sodium fumarate (0.15 g/L), sodium thioglycolate (0.3 g/L), 1% ATCC vitamin solution, and 1% ATCC Trace element solution based on media previously used for human faecal batch culture[60,61]. Faecal cultures with a final concentration of 50 μM bile acids (LCA, 3-oxoLCA, or isoalloLCA) were incubated anaerobically for 48 hr at 37 ºC. DNA was extracted from the faecal sample culture for 16S metagenomic sequencing as described above.

Statistical Analysis

Pairwise Wilcoxon rank-sum test was used to evaluate differences in the relative abundance of *bai* operon homologues in centenarians compared to elderly- and young-controls. Spearman's rank correlation was used to evaluate trends between the relative abundance of Bacteroidales species encoding 5AR, 5BR, 3βHSDH I, or 3βHSDH II genes and the abundance of the secondary bile acids in stool samples. Overall nominal *P*-values were adjusted for multiple testing using Benjamini-Hochberg correction and associations at FDR $P < 0.05$ (unless stated differently) were considered as significant. Statistical analyses below were performed using GraphPad Prism software (GraphPad Software, Inc.). One-way ANOVA with Tukey's test (parametric) and Kruskal-Wallis with Dunn's test (nonparametric) was used for multiple comparisons. Wilcoxon signed-rank test post hoc test with Bonferroni correction (nonparametric) was used to compare group means for meta 16S rRNA analysis. Mann-Whitney test (two-tailed) with Welch's correction (nonparametric) was used for all comparisons between two groups in the co-culture inhibition experiments.

Reporting summary

Further information on experimental design is available in the Nature Research Reporting Summary linked to this article.

Data availability

Shotgun sequencing data will be deposited in NCBI under Bioproject PRJNA675598. Genome sequences of the 68 strains isolated from a centenarian and 16SrRNA amplicon sequence data will be deposited in the DNA Data Bank of Japan.

Acknowledgements We thank Luke Besse for project management and making data available through the SRA and the Broad Institute Genomics Platform and Microbial 'Omics Core for sample processing and sequencing data generation; Akiko Minowa, Mayako Asakawa, and Kayoko Sugita for technical support; Members at JSR-Keio University Medical and Chemical Innovation Center for conducting meta16S rRNA gene sequencing; Miho Shimura and Yukiko Abe for their assistance in collecting clinical samples; Shiota Atsushi and members of Honda laboratory for their helpful suggestions during the course of this studies. Kenya Honda was funded through AMED LEAP under grant number JP20gm0010003, Grant-in-Aid for Specially Promoted Research from JSPS (No: 20H05627), Public/Private R&D Investment Strategic Expansion Program (PRISM) from Cabinet Office of the Government of Japan, the Naito Foundation, and the Takeda Science Foundation. Centenarian study was funded by the Japan Ministry of Agriculture, Forestry, and Fisheries and Keio Global Research Institute (KGRI). The elderly recruitment study was funded by a Grant-in-Aid for Scientific Research (No: 18H03055) from the Japan Society for the Promotion of Science and JST Research Complex Program (JP15667051). D.R.P. and R.J.X. were funded by Center for the Study of Inflammatory Bowel Disease (DK043351) and AT009708. Y.S. was supported by the Terumo Life Science Foundation.

Author Contributions K.H., Y.Sato., and K.A. planned experiments, analysed data, and wrote the paper together with D.R.P., R.J.X., A.N.S., and S.M.K.; Y.A., T.K., and N.H., collected clinical samples; Y.Sato. and K.A. performed bacterial experiments; D.R.P., H.V., and R.J.X. performed metagenome analysis; K.A., S.M.K., Y.O., W.S., and M.H. performed whole genome and meta16S rRNA gene sequencing and analyses; S.Sasajima., Y.Sato., K.A., H.T., H.N., S.N., Y.S., and M.S. performed metabolomic analysis; T.S., S.O., S.Sasajima., and T.M. synthesized chemical compounds; N.M. and S.S. performed electron microscopy imaging; Y.L., T.T., J.I., H.I., and K.M. provided essential materials; D.R.L. and M.A.F. supervised bacterial experiments.

Competing interests K.H. is a scientific advisory board member of Vedanta Biosciences and 4BIO CAPITAL.

719

720 **References**

721 1. Tindale, L. C., Salema, D. & Brooks-Wilson, A. R. 10-year follow-up of the Super-Seniors Study: Compression
722 of morbidity and genetic factors. *BMC Geriatr.* **19**, 58 (2019).

723 2. Arai, Y. *et al.* Inflammation, but not telomere length, predicts successful ageing at extreme old age: A
724 longitudinal study of semi-supercentenarians. *EBioMedicine* **2**, 1549–1558 (2015).

725 3. Andersen, S. L., Sebastiani, P., Dworkis, D. A., Feldman, L. & Perls, T. T. Health span approximates life span
726 among many supercentenarians: Compression of morbidity at the approximate limit of life span. *Journals*
727 *Gerontol. - Ser. A Biol. Sci. Med. Sci.* **67 A**, 395–405 (2012).

728 4. Bárcena, C. *et al.* Healthspan and lifespan extension by fecal microbiota transplantation into progeroid mice.
729 *Nat. Med.* **25**, 1234–1242 (2019).

730 5. Biagi, E. *et al.* Gut microbiota and extreme longevity. *Curr. Biol.* **26**, 1480–1485 (2016).

731 6. Claesson, M. J. *et al.* Gut microbiota composition correlates with diet and health in the elderly. *Nature* **488**,
732 178–184 (2012).

733 7. Rampelli, S. *et al.* Shotgun metagenomics of gut microbiota in humans with up to extreme longevity and the
734 increasing role of xenobiotic degradation. *mSystems* **5**, e00124-20 (2020).

735 8. Wu, L. *et al.* A cross-sectional study of compositional and functional profiles of gut microbiota in Sardinian
736 centenarians. *mSystems* **4**, e00325-19 (2019).

737 9. Nicoletti, C. Age-associated changes of the intestinal epithelial barrier: Local and systemic implications. *Expert*
738 *Rev. Gastroenterol. Hepatol.* **9**, 1467–1469 (2015).

739 10. Huang, Z. & Kraus, V. B. Does lipopolysaccharide-mediated inflammation have a role in OA? *Nat. Rev.*
740 *Rheumatol.* **12**, 123–129 (2016).

741 11. Morais, L. H., Schreiber, H. L. & Mazmanian, S. K. The gut microbiota–brain axis in behaviour and brain
742 disorders. *Nat. Rev. Microbiol.* (2020).

743 12. Franceschi, C., Garagnani, P., Parini, P., Giuliani, C. & Santoro, A. Inflammaging: a new immune–metabolic
744 viewpoint for age-related diseases. *Nat. Rev. Endocrinol.* **14**, 576–590 (2018).

745 13. Santoro, A. *et al.* Microbiomes other than the gut: inflammaging and age-related diseases. *Semin.*
746 *Immunopathol.* (2020).

747 14. Claesson, M. J. *et al.* Composition, variability, and temporal stability of the intestinal microbiota of the elderly.
748 *Proc. Natl. Acad. Sci. U. S. A.* **108**, 4586–4591 (2011).

749 15. Hirata, T. *et al.* Associations of cardiovascular biomarkers and plasma albumin with exceptional survival to the
750 highest ages. *Nat. Commun.* **11**, 1–17 (2020).

751 16. Bloom, D. E. & Cadarette, D. Infectious disease threats in the twenty-first century: Strengthening the global
752 response. *Front. Immunol.* **10**, 549 (2019).

753 17. Lloyd-Price, J. *et al.* Multi-omics of the gut microbial ecosystem in inflammatory bowel diseases. *Nature* **569**,
754 655–662 (2019).

18. Devlin, A. S. & Fischbach, M. A. A biosynthetic pathway for a prominent class of microbiota-derived bile acids. *Nat. Chem. Biol.* **11**, 685–690 (2015).

19. Ridlon, J. M., Kang, D.-J. J. & Hylemon, P. B. Bile salt biotransformations by human intestinal bacteria. *J. Lipid Res.* **47**, 241–259 (2006).

20. Vital, M., Rud, T., Rath, S., Pieper, D. H. & Schlüter, D. Diversity of Bacteria Exhibiting Bile Acid-inducible 7α-dehydroxylation Genes in the Human Gut. *Comput. Struct. Biotechnol. J.* **17**, 1016–1019 (2019).

21. Li, F., Hullar, M. A. J., Schwarz, Y. & Lampe, J. W. Human gut bacterial communities are altered by addition of cruciferous vegetables to a controlled fruit- and vegetable-free diet. *J. Nutr.* **139**, 1685–1691 (2009).

22. Duncan, S. H. *et al.* Reduced dietary intake of carbohydrates by obese subjects results in decreased concentrations of butyrate and butyrate-producing bacteria in feces. *Appl. Environ. Microbiol.* **73**, 1073–1078 (2007).

23. David, L. A. *et al.* Diet rapidly and reproducibly alters the human gut microbiome. *Nature* **505**, 559–563 (2014).

24. De Aguiar Vallim, T. Q., Tarling, E. J. & Edwards, P. A. Pleiotropic roles of bile acids in metabolism. *Cell Metab.* **17**, 657–669 (2013).

25. Wahlström, A., Sayin, S. I., Marschall, H.-U. U. & Bäckhed, F. Intestinal crosstalk between bile acids and microbiota and Its impact on host metabolism. *Cell Metab.* **24**, 41–50 (2016).

26. Funabashi, M. *et al.* A metabolic pathway for bile acid dehydroxylation by the gut microbiome. *Nature* **582**, 566–570 (2020).

27. Ridlon, J. M., Kang, D. J. & Hylemon, P. B. Isolation and characterization of a bile acid inducible 7α-dehydroxylating operon in *Clostridium hylemonae* TN271. *Anaerobe* (2010).

28. Nixon, M., Upreti, R. & Andrew, R. 5α-Reduced glucocorticoids: A story of natural selection. *J. Endocrinol.* **212**, 111–127 (2012).

29. García-Bayona, L. & Comstock, L. E. Streamlined genetic manipulation of diverse *Bacteroides* and *Parabacteroides* isolates from the human gut microbiota. *MBio* **10**, e01762-19 (2019).

30. Hang, S. *et al.* Bile acid metabolites control TH17 and Treg cell differentiation. *Nature* **576**, 143–148 (2019).

31. Campbell, C. *et al.* Bacterial metabolism of bile acids promotes generation of peripheral regulatory T cells. *Nature* **581**, 475–479 (2020).

32. Song, X. *et al.* Microbial bile acid metabolites modulate gut RORγ+ regulatory T cell homeostasis. *Nature* **577**, 410–415 (2020).

33. Brestoff, J. R. & Artis, D. Commensal bacteria at the interface of host metabolism and the immune system. *Nat. Immunol.* **14**, 676–684 (2013).

34. Skelly, A. N., Sato, Y., Kearney, S. & Honda, K. Mining the microbiota for microbial and metabolite-based immunotherapies. *Nat. Rev. Immunol.* **19**, 305–323 (2019).

35. Chen, M. L., Takeda, K. & Sundrud, M. S. Emerging roles of bile acids in mucosal immunity and inflammation. *Mucosal Immunol.* **12**, 851–861 (2019).

36. Buffie, C. G. *et al.* Precision microbiome reconstitution restores bile acid mediated resistance to *Clostridium difficile*. *Nature* **517**, 205–208 (2015).

37. Begley, M., Gahan, C. G. M. & Hill, C. The interaction between bacteria and bile. *FEMS Microbiol. Rev.* **29**, 625–651 (2005).

38. Sung, J. Y., Shaffer, E. A. & Costerton, J. W. Antibacterial activity of bile salts against common biliary pathogens - Effects of hydrophobicity of the molecule and in the presence of phospholipids. *Dig. Dis. Sci.* **38**, 2104–2112 (1993).

39. Urdaneta, V. & Casadesús, J. Interactions between bacteria and bile salts in the gastrointestinal and hepatobiliary tracts. *Front. Med.* **4**, 163 (2017).

40. Thanissery, R., Winston, J. A. & Theriot, C. M. Inhibition of spore germination, growth, and toxin activity of clinically relevant *C. difficile* strains by gut microbiota derived secondary bile acids. *Anaerobe* **45**, 86–100 (2017).

41. Abt, M. C., McKenney, P. T. & Pamer, E. G. *Clostridium difficile* colitis: Pathogenesis and host defence. *Nat. Rev. Microbiol.* **14**, 609–620 (2016).

42. Cushnie, T. P. T., O'Driscoll, N. H. & Lamb, A. J. Morphological and ultrastructural changes in bacterial cells as an indicator of antibacterial mechanism of action. *Cell. Mol. Life Sci.* **73**, 4471–4492 (2016).

43. Piewngam, P. *et al.* Pathogen elimination by probiotic *Bacillus* via signalling interference. *Nature* **562**, 532–537 (2018).

44. Theriot, C. M. *et al.* Antibiotic-induced shifts in the mouse gut microbiome and metabolome increase susceptibility to *Clostridium difficile* infection. *Nat. Commun.* **5**, 3114 (2014).

45. Alavi, S. *et al.* Interpersonal gut microbiome variation drives susceptibility and resistance to Cholera infection. *Cell* **181**, 1533-1546.e13 (2020).

46. Edgar, R. C. Search and clustering orders of magnitude faster than BLAST. *Bioinformatics* **26**, 2460–2461 (2010).

47. Li, D., Liu, C. M., Luo, R., Sadakane, K. & Lam, T. W. MEGAHIT: An ultra-fast single-node solution for large and complex metagenomics assembly via succinct de Bruijn graph. *Bioinformatics* **31**, 1674–1676 (2015).

48. Hyatt, D. *et al.* Prodigal: Prokaryotic gene recognition and translation initiation site identification. *BMC Bioinformatics* **11**, 119 (2010).

49. Fu, L., Niu, B., Zhu, Z., Wu, S. & Li, W. CD-HIT: Accelerated for clustering the next-generation sequencing data. *Bioinformatics* **28**, 3150–3152 (2012).

50. Qin, J. *et al.* A human gut microbial gene catalogue established by metagenomic sequencing. *Nature* **464**, 59–65 (2010).

51. Li, H. & Durbin, R. Fast and accurate short read alignment with Burrows-Wheeler transform. *Bioinformatics* **25**, 1754–1760 (2009).

52. Oñate, F. P. *et al.* MSPminer: Abundance-based reconstitution of microbial pan-genomes from shotgun metagenomic data. *Bioinformatics* **35**, 1544–1552 (2019).

827 53. Li, J. *et al.* An integrated catalog of reference genes in the human gut microbiome. *Nat. Biotechnol.* **32**, 834–
828 841 (2014).

829 54. Segata, N., Börnigen, D., Morgan, X. C. & Huttenhower, C. PhyloPhlAn is a new method for improved
830 phylogenetic and taxonomic placement of microbes. *Nat. Commun.* **4**, 2304 (2013).

831 55. Khelaifia, S., Raoult, D. & Drancourt, M. A versatile medium for cultivating methanogenic archaea. *PLoS One*
832 **8**, e61563 (2013).

833 56. Aziz, R. K. *et al.* The RAST Server: Rapid annotations using subsystems technology. *BMC Genomics* **9**, 75
834 (2008).

835 57. Seemann, T. Prokka: Rapid prokaryotic genome annotation. *Bioinformatics* **30**, 2068–2069 (2014).

836 58. Ferrières, L. *et al.* Silent mischief: Bacteriophage Mu insertions contaminate products of *Escherichia coli*
837 random mutagenesis performed using suicidal transposon delivery plasmids mobilized by broad-host-range RP4
838 conjugative machinery. *J. Bacteriol.* **192**, 6418–6427 (2010).

839 59. Atarashi, K. *et al.* Treg induction by a rationally selected mixture of Clostridia strains from the human
840 microbiota. *Nature* **500**, 232–236 (2013).

841 60. Quinn, R. A. *et al.* Global chemical effects of the microbiome include new bile-acid conjugations. *Nature* **579**,
842 123–129 (2020).

843 61. McDonald, J. A. K. *et al.* Evaluation of microbial community reproducibility, stability and composition in a
844 human distal gut chemostat model. *J. Microbiol. Methods* **95**, 167–174 (2013).

845

Figures

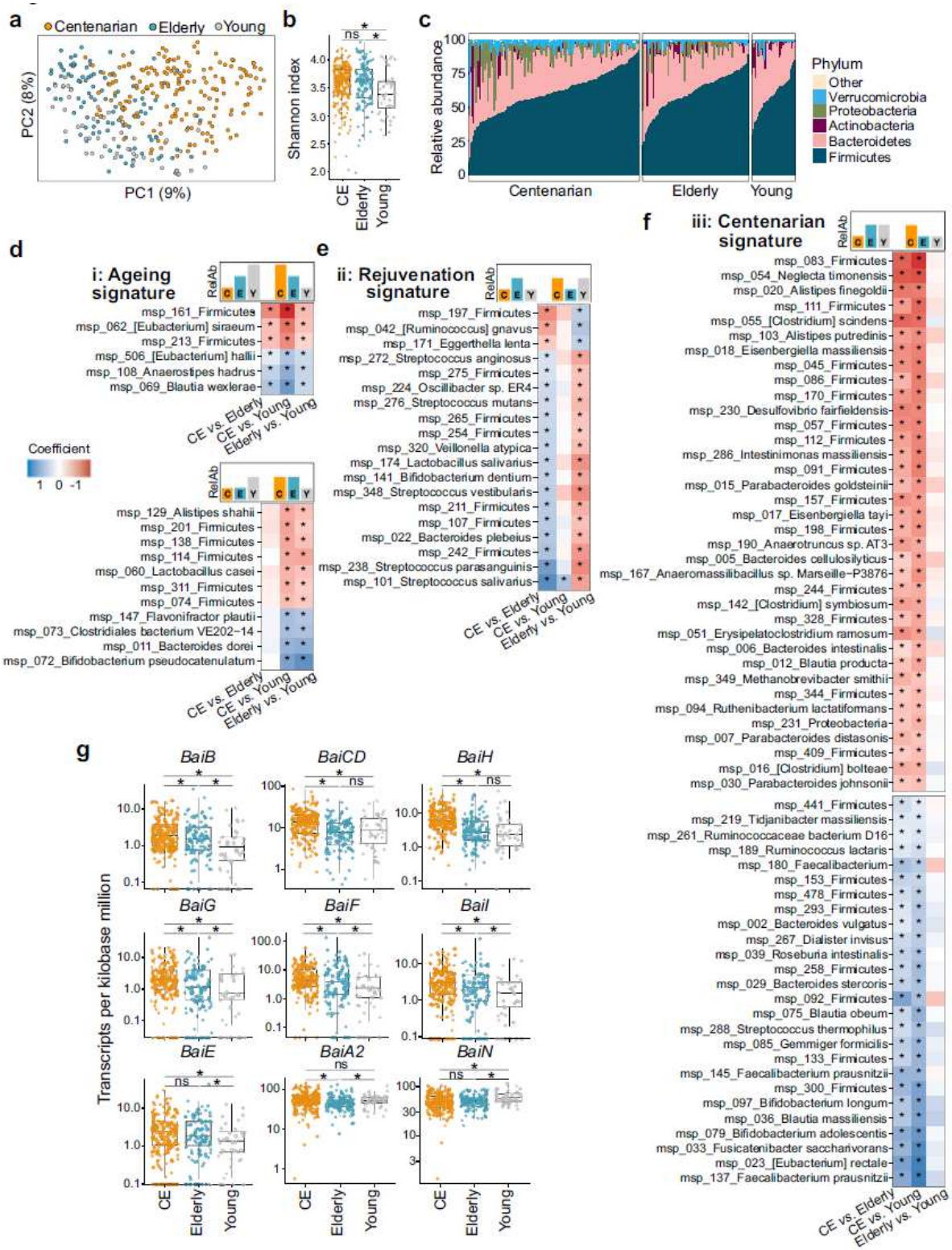

Figure 1

Gut microbiome signatures in centenarian, elderly, and young Japanese subjects based on whole metagenome shotgun sequencing and de novo assembly analysis. a, Principal coordinate analysis based on species-level Bray-Curtis dissimilarity illustrates a gradual separation of centenarian (CE) gut

microbiomes from those of younger subjects. b, Shannon diversity index is significantly increased in centenarians and elderly subjects compared to young subjects ($P < 0.05$, linear model). c, Relative abundance of the five most abundant bacterial phyla. d-f, Changes in the relative abundance (RelAb) of gut microbiome species (MSPs) between centenarian, elderly, and young subjects grouped according to the following signatures of the differential abundance: ageing signature (d), rejuvenation signature (e), and centenarian signature (f). Each signature is accompanied by models depicting examples of different relative abundance for species belonging to a given trajectory in centenarian, elderly, and young age groups. Colour scale represents the coefficient from the linear model and indicates overabundance (red) and depletion (blue) of a species in the respective comparisons: centenarian compared to elderly, centenarian compared to young, and elderly compared to young; in each case, the latter group is used as a reference in the model. Differentially abundant species that are significant at FDR $P < 0.05$ are indicated with asterisks. g, Abundance of homologues to genes from the C. scindens bai operon in centenarian, elderly, and young age groups. Asterisks indicate significant differential abundance in the specified comparison at FDR $P < 0.05$ based on a Wilcoxon rank-sum test. Horizontal lines indicate the median; box boundaries indicate interquartile range (IQR); whiskers represent values within 1.5 x IQR of the first and third quartiles. Centenarian [n = 176 (153 individuals)], elderly (n = 110), and young (n = 44) subjects. Each dot represents one sample.

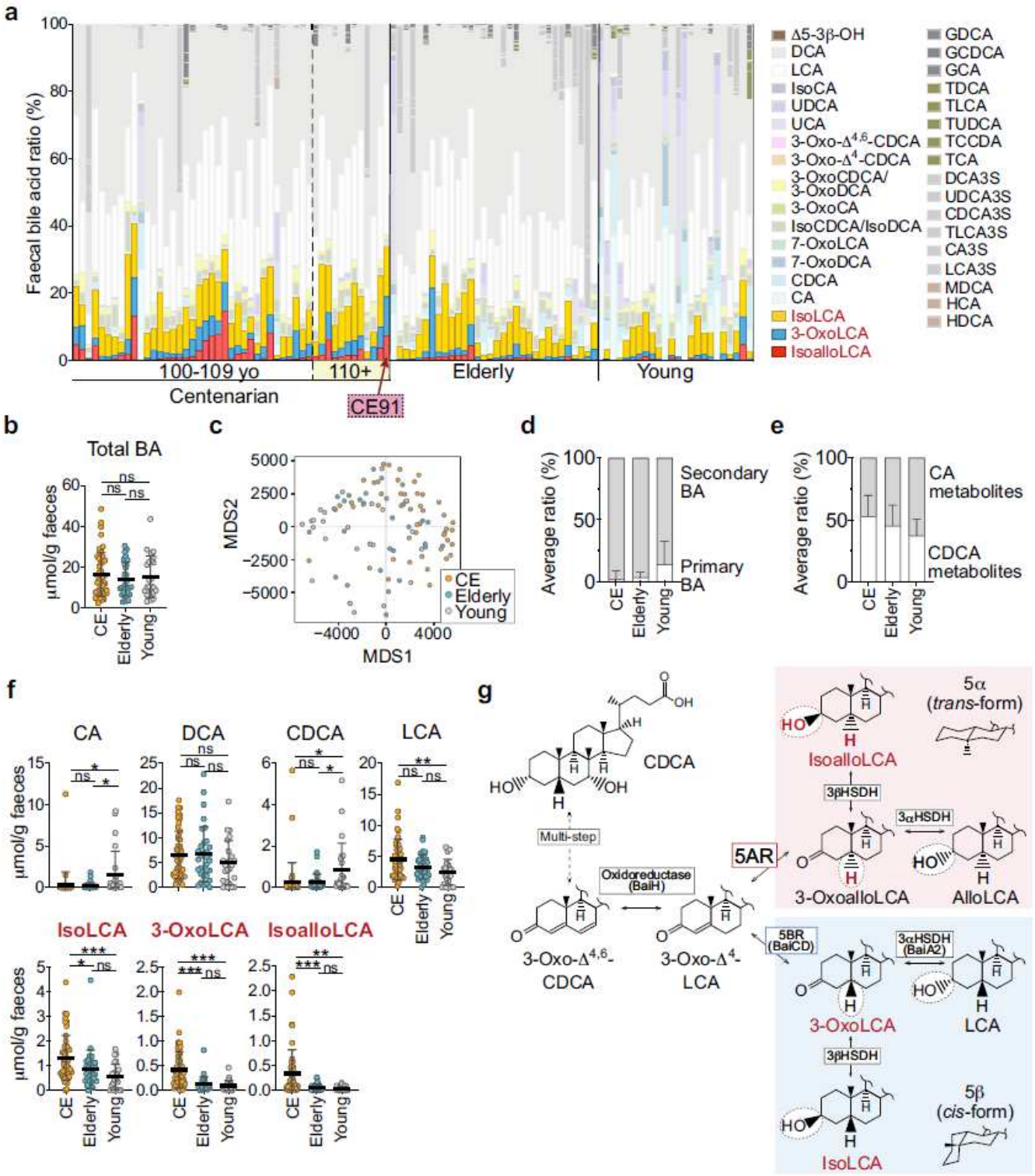

Figure 2

Centenarians have significantly elevated faecal isoLCA, 3-oxoLCA, and isoalloLCA. a, Faecal bile acid compositions of centenarian (n = 49), elderly (n = 32), and young (n = 24) individuals were profiled and quantified by LC-MS/MS. The ratio of isoalloLCA is indicated in red, 3-oxoLCA in blue, and isoLCA in yellow. The results are shown in order of age within each group. Centenarian 91 (CE91), who was selected for follow-up analysis, is labelled. b, Total faecal bile acid (BA) concentration was quantified in

individuals from each of the three age groups. c, Multi-dimensional scaling (MDS) plot using Spearman's correlation highlights differences among the three groups' bile acid profiles. Each dot represents an individual donor coloured by age group. (P = 0.00027 for CE vs. Elderly; P = 1.91E-06 for CE vs. Young; P = 0.027 for Elderly vs. Young; Wilcoxon test). d, e, Average ratio of total primary and secondary (metabolized by gut microbiota) bile acids (d), CA based- (7α- and 12α-OH groups) and CDCA based- (7α-OH group) bile acids (e). f, Quantification of each bile acid compound. g, Simplified biosynthetic pathway for CDCA metabolism by the gut microbiota (see also Extended Data Fig. 5b). Responsible enzymes are indicated within boxes. 5AR, 5α-reductase; 5BR, 5β-reductase; HSDH, hydroxysteroid dehydrogenase. In b, d-f, Data are mean ± s.d. ***P < 0.001; **P < 0.01; *P < 0.05; one-way ANOVA with Tukey's test. ns, not significant. Each dot represents an individual. Faecal total bile acids are shown in μmol/g dry weight faeces.

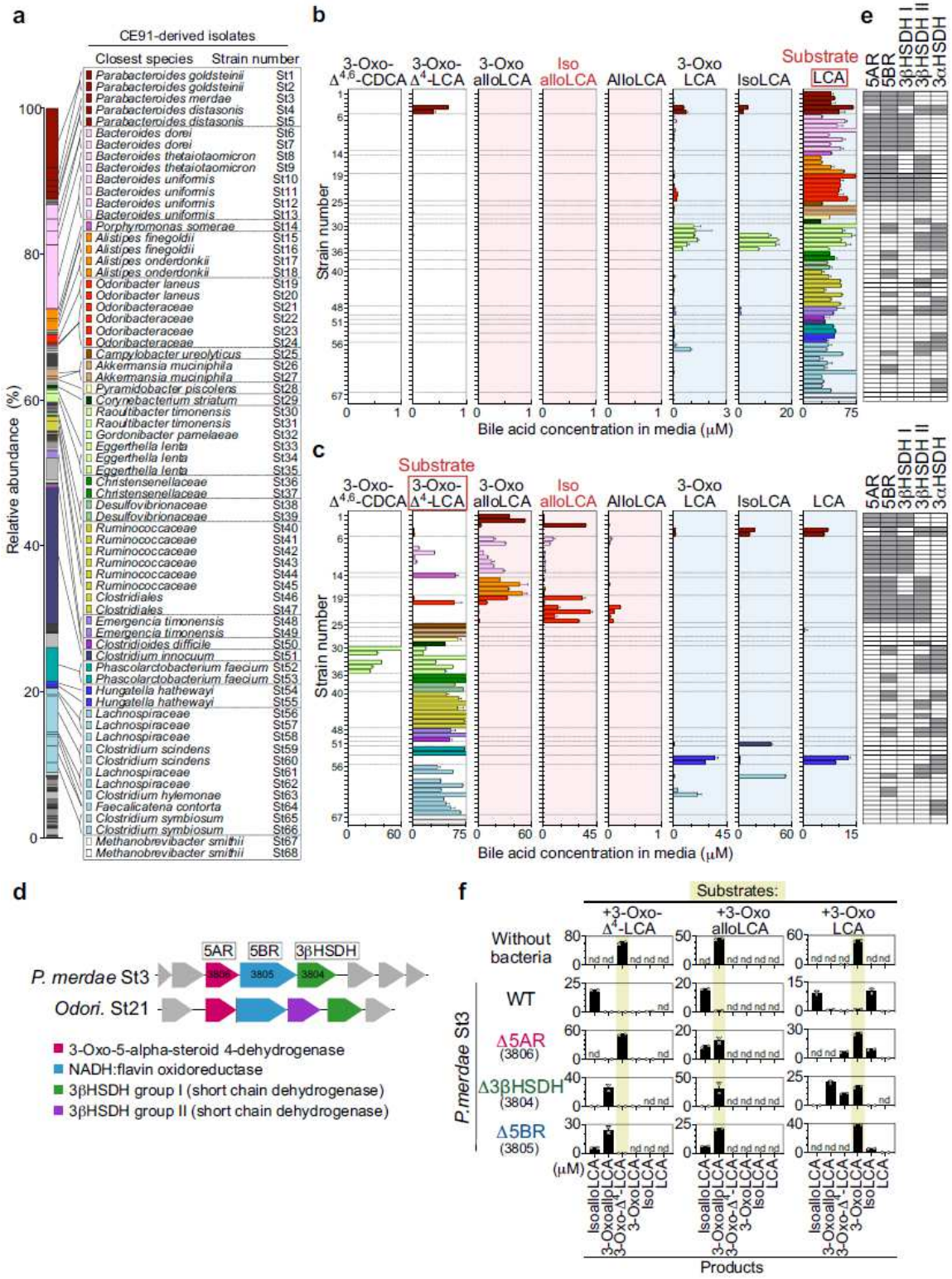

Figure 3

Identification of bacterial strains and genes involved in generation of isoLCA, 3-oxoLCA, and isoalloLCA. a, Faecal microbial composition of CE91 aligned with a list of 68 isolated strains. b, c, In vitro bile acid metabolism by the 68 CE91-derived strains using 50 μM of LCA (b) and 3-oxo-Δ4-LCA (c) as starting substrates (see also Extended Data Fig. 8). Isolated strains were cultured anaerobically in media adjusted to pH 9 for 48 hr at 37 □. Graph with red backgrounds indicate trans-form bile acids, while those with blue

background indicate cis-form bile acids. d, Schematic drawings of predicted bile acid-metabolizing enzyme genes in P. merdae St3 and Odoribacteraceae St21. Arrows represent coding sequences and annotated functions are coloured accordingly. e, Predicted bile acid-metabolizing enzyme genes from corresponding isolates. Presence of genes homologous to 5AR, 5BR, 3βHSDH (3βHSDH I; 3βHSDH II), and 3αHSDH in corresponding strains are indicated. Gene homologues were defined as <1e-12 E-value; >30% identity; >60% query coverage. f, Bile acid metabolism assay in P. merdae St3 knockout strains of 5AR (magenta), 3βHSDH (green), or 5BR (blue) genes. 50 μM of 3-oxo-β4-LCA, 3- oxoalloLCA, or 3-oxoLCA were added as starting substrates in pH 9-adjusted medium and incubated for 48 hr at 37 □. Yellow shading indicates detected concentrations of starting substrates. nd, not detected. In b, c, and f, Bile acid concentrations were determined by LC-MS/MS and data are mean ± s.d. of duplicate samples.

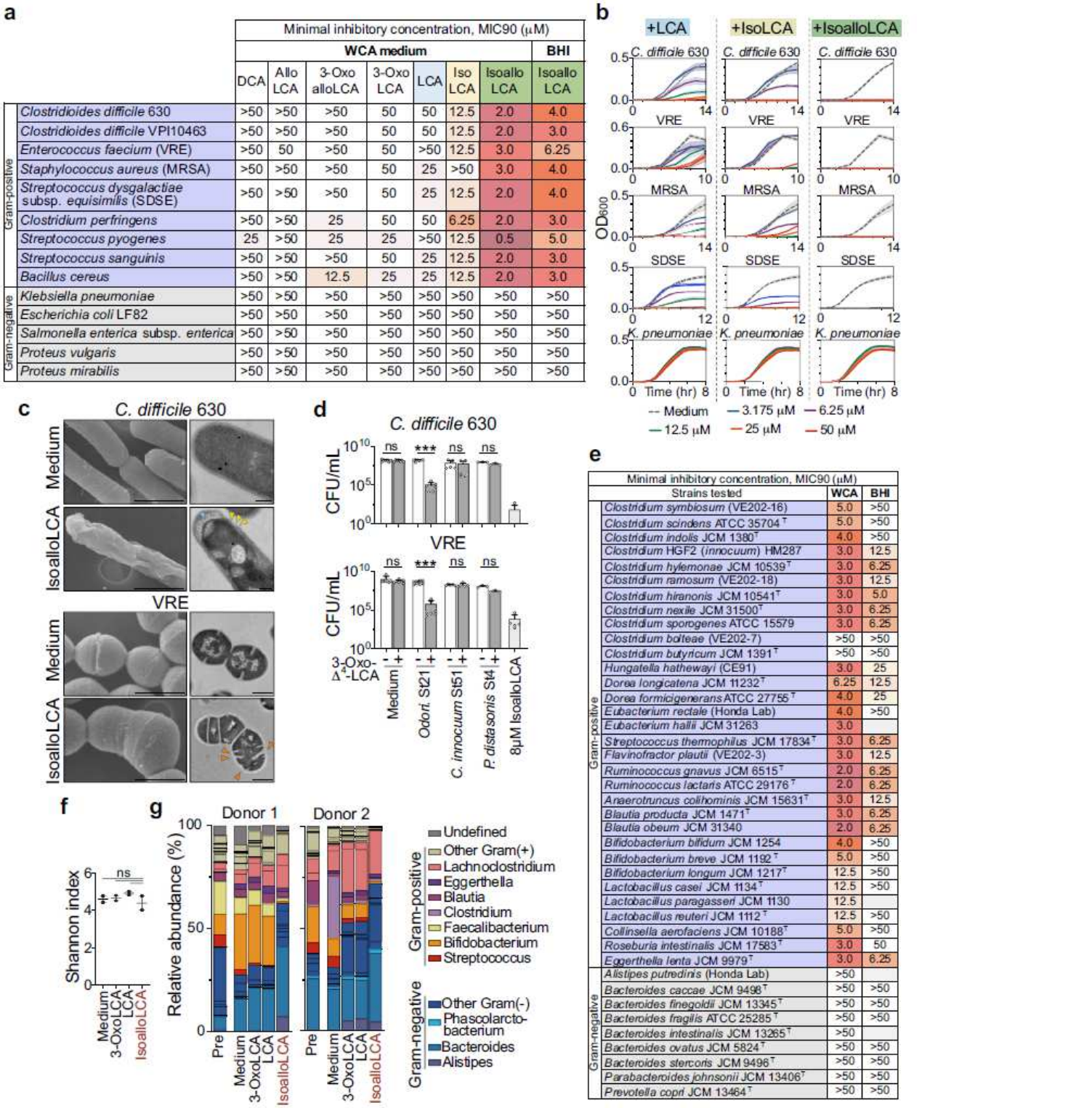

Figure 4

IsoalloLCA exerts potent antimicrobial activity against gram-positive pathogens. a, Minimal inhibitory concentration required to prevent 90% growth (MIC90) of secondary bile acids against grampositive and gram-negative pathogens in Wilkins-Chalgren Anaerobe (WCA) and Brain Heart Infusion (BHI) broth media. b, Growth curves of pathogens in varying concentrations of LCA (blue), isoLCA (yellow), and isoalloLCA (green) in WCA medium. Data are mean ± s.d. (error bars shown with fill area). c,

Representative scanning (SEM, left panels) and transmission (TEM, right panels) electron microscopy images of C. difficile 630 and VRE grown in WCA medium with or without 8 μM isoalloLCA for 5 hr. Scale bars are 1.0 μm (SEM), 200 nm (C. difficile 630 TEM), or 500 nm (VRE TEM). Arrows indicate morphological alternations following isoalloLCA treatment. d, In vitro growth inhibition of C. difficile 630 and VRE by co-culturing with CE91-derived Odoribacteraceae St21, C. innocuum St51, or P. distasonis St4 in the presence or absence of 12.5 μM of 3-oxo-Δ4-LCA in WCA medium. Average CFU of overnight cultures are shown (n = 6). e, IsoalloLCA MIC90 on commensal strains in WCA and BHI media. f, g, Human faecal samples from healthy young donors were incubated for 48 hr in a modified WCA medium supplemented with 3-oxoLCA, LCA, or isoalloLCA (50 μM). Shannon index of diversity (f) and a compositional shift in the microbiome at the genus level (g) of faecal cultures after secondary bile acid treatment. In d, f, Data are mean ± s.d. ***P < 0.001; Mann-Whitney test (two-tailed) with Welch's correction (d) or Kruskal- Wallis with Dunn's test (f). ns, not significant. Each circle represents one co-culture sample (d) or the donor's faecal culture (f).

Supplementary Files

This is a list of supplementary files associated with this preprint. Click to download.

- TableS1.xlsx
- TableS2.xlsx
- TableS3.xlsx
- TableS4.xlsx
- SIfigs.pdf